AIP | The Journal of Chemical Physics

Dynamics of two interacting active Janus particles

Parvin Bayati and Ali Najafi

Citation: The Journal of Chemical Physics **144**, 134901 (2016); doi: 10.1063/1.4944988
View online: http://dx.doi.org/10.1063/1.4944988
View Table of Contents: http://scitation.aip.org/content/aip/journal/jcp/144/13?ver=pdfcov
Published by the AIP Publishing

Dynamics of two interacting active Janus particles

Parvin Bayati[1] and Ali Najafi[1,2,a)]
[1]*Physics Department, University of Zanjan, Zanjan 45371-38791, Iran*
[2]*Department of Physics, Institute for Advanced Studies in Basic Sciences (IASBS), Zanjan 45137-66731, Iran*

(Received 27 October 2015; accepted 17 March 2016; published online 4 April 2016)

Starting from a microscopic model for a spherically symmetric active Janus particle, we study the interactions between two such active motors. The ambient fluid mediates a long range hydrodynamic interaction between two motors. This interaction has both direct and indirect hydrodynamic contributions. The direct contribution is due to the propagation of fluid flow that originated from a moving motor and affects the motion of the other motor. The indirect contribution emerges from the re-distribution of the ionic concentrations in the presence of both motors. Electric force exerted on the fluid from this ionic solution enhances the flow pattern and subsequently changes the motion of both motors. By formulating a perturbation method for very far separated motors, we derive analytic results for the translation and rotational dynamics of the motors. We show that the overall interaction at the leading order modifies the translational and rotational speeds of motors which scale as $O\left([1/D]^3\right)$ and $O\left([1/D]^4\right)$ with their separation, respectively. Our findings open up the way for studying the collective dynamics of synthetic micro-motors. © *2016 AIP Publishing LLC.* [http://dx.doi.org/10.1063/1.4944988]

I. INTRODUCTION

Designing the synthetic micro-propelling systems with an ability to navigate in predefined and controllable trajectories is the aim of many researchers in both chemistry and physics.[1] Delivery of drug at living systems and construction of manipulating tools for lab on chip experiments are among the main applications of such systems. Hydrodynamic swimmers,[2–4] single DNA molecule propeller,[5] light mediated motion of Janus particles in binary mixtures and colloidal systems,[6,7] and phoretic propulsion of spheroidal particles[8] are most recent proposed designs for micro-machines.

Apart from their potential applications as listed above, the physics of directed motion at the scale of micrometer is also a challenging issue in physics.[9,10] This is mainly due to the inertia-less condition that constrains the physics at this scale. At macroscopic scale of the daily life, inertia provides a mechanism for movements, but at microscopic scale, the life is dominated by dissipation. As a result of this ambiguity, a backward ejection of a high-speed jet of molecules is not able to propel a micron size boat. For driving a micrometer boat, we need to go beyond our macroscopic feeling of motion and use nontrivial mechanisms for swimming strategies.[2,11,12]

Janus particles with surface chemical activity are the potential proposals for cargo delivery machines at the scale of micrometer. Originated from a very interesting experiment by Paxton *et al.*,[13,14] a great deal of the researcher's attention has been attracted by the idea of generating directed motion by surface reactions.[15–18] As a recent example, Janus particles made from spherical Pt insulator have been studied extensively.[19,20] Drug delivery[21–26] and ability for entering into cells by catalytic Janus particles[27] have been examined experimentally. Another interesting application of catalytic micro-motors includes water purification that has been successfully tested.[28,29] Also it is shown that using Janus particles, one can make a chemical sensor.[30] Understanding and predicting the physical behavior of a single or many such motors constitute the core of many recent researches.[31]

The physics of a single Janus particle propeller has been investigated theoretically[32] and numerically.[33–35] Recently, motion of Janus self-propellers in different conditions has been considered. This includes dynamic of a particle confined by a planar wall and also motion in shear flow. It is shown that depending on the initial state of a Janus particle, a rigid and electrically neutral wall can both attract or repel a nearby Janus motor.[36,37] The dynamical response of a Janus motor moving in an ambient shear flow have a crucial dependence on the strength of thermal fluctuations of the ions.[38]

For most of the expected applications of micro-machines, it is reasonable to use a collection of them to achieve maximum efficiency. Along this task, one needs to have an understanding of the physics of mutual interaction between two or many of Janus motors. Such theoretical knowledge will allow the researchers to predict the collective behavior of a suspension of many Janus motors system. So far and up to our knowledge, all theoretical works are limited to the physics of individual motors. In this article, we address the problem of interaction between two self-propelled Janus motors.

A number of interesting phenomena in a system of two or many hydrodynamical swimmers have been observed. These include a class of phenomena ranging from coherent motion of two coupled swimmers[39–41] to pattern formation and reduction of effective viscosity in suspensions.[42–46] Inspiring from these hydrodynamical systems, we expect to see a rich physical behavior in the case of Janus particles which are electro-hydrodynamical and in addition to hydrodynamic effects, the presence of long range electrostatic forces should also be considered.

a)Electronic mail: najafi@znu.ac.ir

The rest of this article organizes as follows: in Section II, we introduce the system and write the basic governing equations. Sections III and IV are devoted to develop the approximations that we will use. Analytic results for a single motor are collected in Section V and the problem of interacting particles is presented in Section VI. Finally, discussion about our results is presented in Section VII.

II. GOVERNING EQUATIONS

We start by analyzing the physics of a single motor that benefits surface chemical reactions to propel itself. A schematic view of the model system that we are interested to analyze is shown in Figure 1. A charged colloidal particle with radius a and electrostatic surface potential given by ψ_s is immersed in an electrolyte solution with electric permeability ε_r and hydrodynamic viscosity η. Solution consists of two ionic species, cations and anions with valances given by $Z_\pm$, respectively (throughout this paper, + refers to cations and − refers to anions). We consider the simple case where the electrolyte is symmetric and single valence with $Z_+ = -Z_- = 1$. Driving force of this motor emerges from an asymmetric surface chemical activity. We assume that the surface properties of the motor allow it to absorb and emit chemical species in an asymmetric way. As shown in figure, the north hemisphere of the Janus particle can emit ionic particles, either cations or anions. The south hemisphere of the Janus particle can absorb the ions with the same rate given at the emitting part. Such a simple modeling can take into account the physics of most experimentally realized Janus motors.

We use dimensionless units to introduce the dynamical equations. In addition to simplifying the notations, dimensionless form of the equations will help us to introduce our approximate scheme for solving the equations. We will use the radius of the motor a, potential associated with thermal energy $\psi_0 = (k_B T/e)$, and equilibrium concentration of ions at infinity n_∞, to make non-dimensional form for all length scales, electric potential, and concentrations, respectively. A velocity scale given by $v_0 = (k_B T/e)^2(\varepsilon_r/\eta a)$ and a characteristic pressure $p_0 = v_0\eta/a$ will be used to make the velocities and pressures non-dimensional. One should note that such dimensional analysis is not unique, we are using the one that may work efficiently, it can capture the most important part of the physics, and it also makes the presentation more simpler.

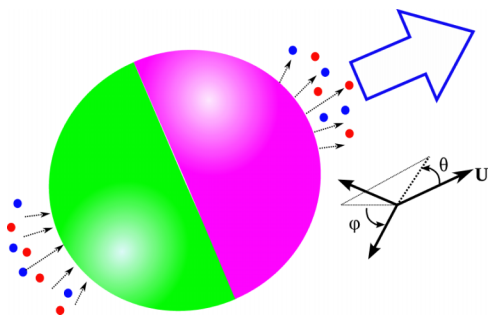

FIG. 1. A spherical micron size particle benefits surface reactions to propel itself. Surface activity of the particle allows both production and absorption of ionic molecules. With respect to a co-moving reference frame, an azimuthally symmetric but polar pattern of surface activity is able to produce a net propulsion.

Denoting the ionic fluxes of cations and anions by $\mathbf{j}_\pm(\mathbf{x})$, we consider a prescribed surface activity given by the following condition on the surface of motor:

$$\hat{\mathbf{n}} \cdot \mathbf{j}_\pm(\mathbf{r} = \hat{\mathbf{n}}) = \dot{Q}\cos\theta, \tag{1}$$

where $\mathbf{j}_\pm(\hat{\mathbf{n}}) = \mathbf{j}_\pm^s$ shows the flux of ions given on the surface of the spherical Janus particle. In the above equation, $\dot{Q}$ is a constant ionic rate, θ is the azimuthal angle with respect to a fixed $z-$axes co-moving with the motor, and $\hat{\mathbf{n}}$ represents a unit vector that is normal to the surface. For the above model of surface activity, total number of both ionic species in the solution are fixed. In physical systems like the one that was studied by Paxton *et al.*, neutral molecules coming from infinity catalyze on the surface of motor and provide the source of surface ionic flux. In addition to the above mentioned catalytic realization of our model, it can also be considered as a motor that works base on an osmotic pressure difference between the inside and outside of the motor. Here we want to neglect the complexities associated with the motion of species before reaching the catalytic points on the surface of motor and simplify the system. We assume that the interior of motor is a source of ions. These ions can diffuse outside from the permeable surface of the motor. One can consider a sphere that is constructed by a semi-permeable membrane. An internal active compartment inside the motor provides an angle dependent osmotic pressure difference between inside and outside of the motor. Due to this pressure difference, the above surface ionic flow can appear in the system. However, our results can also be used to understand the most physical behavior of the phoretic motors with fuel coming from infinity. This is mainly due to the fact that the fluid motion at very far distances from the motor has no contribution on the speed of motor. It is only the electrokinetic effects very near to the motor surface that determine the overall behavior of motor. Fuel molecules coming from infinity, before reaching the catalytic cites on the motor, are neutral and therefore have no electric effect. This ensures us that whether the fuel molecules come from infinity or from the interior of motor, they will provide approximately same driving forces.

As a result of this asymmetric surface property, the motor will achieve a constant steady state propulsion velocity. We would like to calculate this propulsion velocity as a function of the physical properties of the motor and the electrolyte characteristics.

Simultaneous solution to the hydrodynamic equations and the electrostatic equations for the ionic concentrations will reveal the propulsion velocity. These two sets of equations are coupled via the hydrodynamic body force that appears in the hydrodynamic equations. As discussed before, the hydrodynamics of a micron scale system should be described by governing equations at very small inertia condition. This is a condition given by very small Reynolds number, $\mathcal{R}e \ll 1$. Neglecting the inertial effects, the Stokes equation governs the dynamics of the fluid at fully dissipative limit,[47]

$$\nabla^2\mathbf{u}(\mathbf{r}) - \nabla p(\mathbf{r}) = -(n_+(\mathbf{r}) - n_-(\mathbf{r}))\nabla\psi(\mathbf{r}), \tag{2}$$

where $\mathbf{u}(\mathbf{r})$ and $p(\mathbf{r})$ stand for velocity and pressure field of the fluid. Assuming that the fluid is in-compressible, the velocity field should satisfy a continuity equation as $\nabla \cdot \mathbf{u}(\mathbf{r}) = 0$. Right hand side of the Stokes equation represents an electric body force acting on the fluid that comes from the ions, where $n_{\pm}(\mathbf{r})$ and $\psi(\mathbf{r})$ are ionic concentrations and electric potential of the ions. The electrostatic potential satisfies the Poisson-Boltzmann equation,

$$\delta^2 \nabla^2 \psi = -\frac{1}{2}(n_+ - n_-). \tag{3}$$

Continuity equations for the ionic currents are another equations that should be satisfied. The continuity equations for ions read

$$\frac{\partial n_{\pm}(\mathbf{r})}{\partial t} + \nabla \cdot \mathbf{j}_{\pm}(\mathbf{r}) = 0. \tag{4}$$

Thermal fluctuations of the ions, drift due to the electric forces and convection due to the flow of fluid, are different sources for the ionic currents. Collecting all these terms, we can write the following phenomenological relations for the ionic currents as

$$\mathbf{j}_{\pm}(\mathbf{r}) = -\nabla n_{\pm}(\mathbf{r}) \mp n_{\pm}(\mathbf{r}) \nabla \psi(\mathbf{r}) + \mathcal{P}e\, n_{\pm}(\mathbf{r}) \mathbf{u}(\mathbf{r}), \tag{5}$$

where the phenomenological contribution from the fluctuations is expressed in terms of the concentration gradient.

Two important dimensionless numbers, δ and $\mathcal{P}e$ that are appeared in governing equations, are given by

$$\delta^2 = 1/(\kappa a)^2 = \frac{\varepsilon_r k_B T}{2e^2 n_\infty a^2}, \quad \mathcal{P}e = \frac{\varepsilon_r (k_B T)^2}{\eta e^2 \mathcal{D}}. \tag{6}$$

Debye screening length δ measures the equilibrium thickness of ionic cloud around a colloid which is immersed in an ionic solution. This is essentially a length beyond which the electric effects of the colloid are screened. Peclet number $\mathcal{P}e$ measures how the convection is effective in comparison with thermal diffusion. For very small Peclet number, the current due to the thermal fluctuations is dominated over the current from convection. In our description of the system, and for mathematical simplifications, the diffusion constants for both ions are assumed to be equal and we denote both of them by $\mathcal{D}$. In general, the ionic diffusion constants depend on the size of ions, which results in a different value for cations and anions. As we are not interested about the phenomena that could result from such asymmetry between cations and anions, we restrict ourselves to the symmetric case with equal diffusion constants.

In addition to the boundary condition given by Equation (1), there are other boundary conditions that should be considered. On the surface of motor and in a co-moving frame, the boundary conditions for the fluid velocity and ionic potential read

$$\mathbf{u}(\mathbf{r}) = 0, \quad \psi(\mathbf{r}) = \psi_s, \quad \mathbf{r} = a\hat{\mathbf{n}}.$$

Very far from the motor, at $r \to \infty$, the boundary conditions read

$$\mathbf{u}(\mathbf{r}) = -\mathbf{U}, \quad \nabla\psi(\mathbf{r}) = 0, \quad \psi(\mathbf{r}) = 0, \quad n_{\pm} = n_\infty,$$

where $\mathbf{U}$ is the propulsion velocity of the motor that needs to be determined by solving the above equations. As the motor propulsion is not due to any external force, total force acting on the motor vanishes. Collecting both the hydrodynamic and electrostatic forces acting on the spherical motor, the force free condition can be written as

$$\mathbf{F} = \oint_S \Big\{ -p\mathbb{I} + \nabla\mathbf{u} + (\nabla\mathbf{u})^T + \nabla\psi\nabla\psi - \frac{1}{2}\nabla\psi \cdot \nabla\psi \mathbb{I} \Big\} \cdot \hat{\mathbf{n}}\, dS = 0, \tag{7}$$

where $\mathbb{I}$ refers to the 3×3 unit matrix, and superscript T refers to transpose of a square matrix.

For a typical experiment that we are interested, a micron sized particle with $a \sim 1\ \mu$m moves in an electrolyte solution with $\eta \sim 10^{-3}$ Pa s, $\mathcal{D} = \times 10^{-9}$ m^2/s, and $n_\infty = 10^{23}$ m^{-3} (data are given for 0.001M solution of KCL at room temperature).[48] In this case, we will have $\delta \sim 10^{-3}$ and $\mathcal{P}e \sim 10^{-1}$. For a typical system with these numerical values for physical parameters, we can proceed by applying the condition $\delta \ll 1$ to the dynamical equations and obtain approximate analytic results. In the limit of strong electrostatic screening and also small convection, we expect to have great simplifications in dynamical equations.

III. THIN DEBYE LAYER, $\kappa a \gg 1$

In the limit of thin Debye layer with $\delta \to 0$, it can be concluded from Equation (3) that

$$n_+ = n_- = N. \tag{8}$$

As a result of the singularity at the limit of $\delta = 0$, the above electro-neutrality condition can be applied only at the outside of Debye layer. The Debye layer is a thin screening layer adjacent to the surface of Janus particle. One should note that the concept of Debye layer works only for a system that is in equilibrium. The flux of ions in the surface of the motor may violate the criteria of equilibrium. For a very thin Debye layer and small value for ionic flux, we do not expect to see any observable distortion in Debye layer. To be more quantitative, Damkohler dimensionless number should be calculated. This dimensionless number determines whether the system is in equilibrium or not. This number compares the reaction rate of ions on the surface of the motor with the diffusion rate as $\mathcal{D}_a = (\dot{Q}a)/(\mathcal{D}n_\infty)$. We assume that $\mathcal{D}_a \ll 1$ to guarantee that neglecting non-equilibrium features is reasonable.

At this condition and to study the physical properties of the system, we use a macroscale description developed by Yariv and co-workers.[49,50] In such description, by decomposing the space into the Debye-layer and the region outside of it (bulk region), one aims to extract an effective macroscale properties of the electro-neutral bulk region. Such effective fields will provide approximations to the real bulk properties of the system. The physics inside the Debye layer is governed by the equilibrium Boltzmann distribution for the ionic concentrations. Effective physical properties at the bulk can be achieved by applying effective proper boundary conditions on outer surface of the Debye layer on macroscale fields (instead of the application of boundary conditions on the particle surface). Denoting the effective bulk fields by capital

letters, we need to solve the following governing equations for hydrodynamics in the bulk:

$$\nabla^2\mathbf{V} - \nabla P + \nabla^2\Psi\nabla\Psi = 0, \quad \nabla\cdot\ \mathbf{V} = 0, \tag{9}$$

and also the ionic properties are given by the solutions to the following equations:

$$\nabla^2 N - \mathcal{P}e\ \mathbf{V}\cdot\nabla N = 0, \quad \nabla\cdot(N\nabla\Psi) = 0. \tag{10}$$

The effective fields obviously satisfy the same boundary conditions as real microscopic fields at infinity. However, the boundary conditions on the particle surface will change to the boundary conditions given on the Debye layer. Combining the boundary condition given in Equation (1) by the definition for the current density given by Equation (5), we arrive at the following boundary conditions on the surface ($\mathbf{r} = \hat{\mathbf{n}}$):

$$\frac{\partial N}{\partial n} = -\dot{Q}\cos\theta, \quad \frac{\partial\Psi}{\partial n} = 0, \quad \Psi = \psi_s - \zeta, \tag{11}$$

where ζ is the electric potential drop between the particle surface and the outer surface of Debye layer and ψ_s is the surface potential of the particle. For full screening limit, $\zeta = \psi_s$. A significant and most important part of the boundary conditions on outer surface of Debye layer is that of a slip velocity condition that is known as the Dukhin-Derjaguin slip velocity on the effective velocity field given by[51]

$$\mathbf{V}_S = \zeta\nabla_S\Psi - 4\ln\left(\cosh\frac{\zeta}{4}\right)\nabla_S\ln N, \qquad \mathbf{r} = \hat{\mathbf{n}}, \tag{12}$$

where $\frac{\partial}{\partial n} = \hat{\mathbf{n}}\cdot\nabla$ and $\nabla_S = (\mathbb{I} - \hat{\mathbf{n}}\hat{\mathbf{n}})\cdot\nabla$ is the surface gradient. Here S shows the outer surface of Debye layer.

In the passive case, where the surface of particle is not active, $\dot{Q} = 0$ and the above equations have trivial equilibrium solutions given by

$$N = 1, \quad \Psi = 0, \quad P = 0, \quad \mathbf{V} = 0, \quad \zeta = \text{constant}. \tag{13}$$

Obviously for a passive particle, the propulsion velocity vanishes $\mathbf{U} = 0$. We expect to obtain non-zero self-propulsion velocity for a particle with surface activity.

IV. SMALL SURFACE ACTIVITY

Although the thin Debye layer approximation makes the equations very simpler, but they are still highly coupled and it is not possible to present analytic solutions. This difficulty can be overcome by considering the case where the surface activity of the motor is weak. For very small value of $\dot{Q}$, we can present a systematic expansion in powers of $\dot{Q}$. Expanding all variables in terms of $\dot{Q}$, we have

$$\begin{aligned} &N = 1 + \dot{Q}N' + O(\dot{Q})^2, \quad \Psi = \dot{Q}\Psi' + O(\dot{Q})^2,\\ &P = \dot{Q}P' + O(\dot{Q})^2, \qquad \mathbf{V} = \dot{Q}\mathbf{V}' + O(\dot{Q})^2, \end{aligned} \tag{14}$$

and

$$\begin{aligned} \zeta &= \zeta_0 + \dot{Q}\zeta' + O(\dot{Q})^2, \ \ \psi_s = \zeta_0 + \dot{Q}\psi_s' + O(\dot{Q})^2,\\ \mathbf{U} &= \dot{Q}\mathbf{U}' + O(\dot{Q})^2. \end{aligned} \tag{15}$$

Up to the first order in small quantity $\dot{Q}$, the dynamical equations read

$$\begin{aligned} &\nabla^2 N' = 0, \qquad \nabla^2\Psi' = 0,\\ &\nabla^2\mathbf{V}' = \nabla P', \qquad \nabla\cdot\mathbf{V}' = 0. \end{aligned} \tag{16}$$

These equations should be solved provided the following boundary equations at the outer surface of Debye layer, $\mathbf{r} = \hat{\mathbf{n}}$:

$$\begin{aligned} &\Psi' = \psi_s' - \zeta', \quad \frac{\partial N'}{\partial n} = -\cos\theta, \quad \frac{\partial\Psi'}{\partial n} = 0,\\ &\mathbf{V}' = \zeta_0\nabla_S\Psi' - 4\ln\left(\cosh\frac{\zeta_0}{4}\right)\nabla_S N'. \end{aligned} \tag{17}$$

The boundary conditions at $\mathbf{r}\to\infty$ are given by

$$N' = 0, \qquad \nabla\Psi' = 0, \qquad \mathbf{V}' = -U'\hat{\mathbf{z}}. \tag{18}$$

One should note that the force free condition at the first order of $\dot{Q}$ reads

$$\mathbf{F}' = \oint_{r=1}\left\{-P'\mathbb{I} + \nabla\mathbf{V}' + (\nabla\mathbf{V}')^T\right\}\cdot\hat{\mathbf{n}}\ dA = 0. \tag{19}$$

As a result of the above calculations, one can see that in the limit that we work, the electrostatic effects have no contribution in the total force.

In the following parts, we first derive the propulsion velocity and also the velocity field due to a single motor. Then the problem of interacting motors will be addressed in detail.

V. SINGLE JANUS PARTICLE

Here, we calculate the properties of a single motor in the limits that described before. As N' and Ψ' simply satisfy the Poisson equation, their azimuthal symmetric solutions can be written as an expansion in terms of Legendre polynomials,

$$\begin{aligned} \Psi'(r,\theta) &= \sum_m \left(A_m r^m + B_m r^{-(m+1)}\right) P_m(\cos\theta),\\ N'(r,\theta) &= \sum_m \left(A'_m r^m + B'_m r^{-(m+1)}\right) P_m(\cos\theta). \end{aligned} \tag{20}$$

Applying the boundary conditions and up to the leading order of $\dot{Q}$, the following unique solutions can be derived:

$$N' = \frac{1}{2r^2}\cos\theta, \quad \Psi' = \psi_s - \zeta = \text{constant}. \tag{21}$$

Having in hand the ionic concentration, we can proceed to calculate the hydrodynamical variables as well. As a result of symmetry considerations, we assume that the self propelled velocity of the particle points along the $\hat{\mathbf{z}}$ direction. So we can put $\mathbf{U}' = U'\hat{\mathbf{z}}$ and search for the value of U'. Using the above result for the concentration profile, the slip velocity on the particle surface can be written down as

$$\begin{aligned} \mathbf{V}'_S &= -4\ln\left(\cosh\frac{\zeta_0}{4}\right)\nabla_S N'|_{r=1}\\ &= 2\ln\left(\cosh\frac{\zeta_0}{4}\right)\sin\theta\ \hat{\boldsymbol{\theta}}. \end{aligned} \tag{22}$$

In addition to the above conditions, the force free condition should also be considered.

In order to evaluate the particle velocity U', we proceed by applying the well known reciprocal theorem of low Reynolds

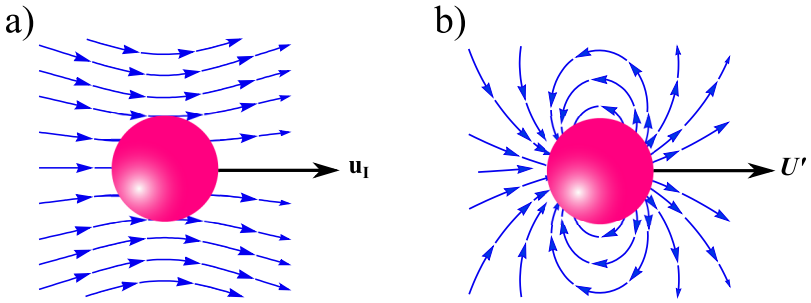

FIG. 2. Two different hydrodynamic problems are used in reciprocal theorem to achieve the swimming velocity of a Janus particle. (a) Problem I: the velocity field of a translating sphere with velocity $u_I\hat{\mathbf{z}}$, (b) problem II: the velocity field of a self propelling Janus particle with slip velocity given by Equation (22), in laboratory reference frame.

hydrodynamics.[52] The Lorentz reciprocal theorem relates the solutions of two distinct Stokes flow problems which share the same geometry but having different boundary conditions. According to this theorem, the velocity fields $\mathbf{V}_I$ and $\mathbf{V}_{II}$ and also the corresponding stresses $\boldsymbol{\sigma}_I$ and $\boldsymbol{\sigma}_{II}$ of two problems are related by a surface integral over domain boundaries as

$$\int \mathbf{V}_I \cdot \boldsymbol{\sigma}_{II} \cdot \hat{\mathbf{n}}\, dS = \int \mathbf{V}_{II} \cdot \boldsymbol{\sigma}_I \cdot \hat{\mathbf{n}}\, dS. \tag{23}$$

The integral is over a surface that defines the boundary. The velocity profiles $\mathbf{V}_I$ and $\mathbf{V}_{II}$ are subjected to different boundary conditions on the surface and both of them are assumed to vanish at infinity.

Here and to use the reciprocal theorem for extracting the swimming velocity of Janus particle, we choose problems I and II as follows. For case I, we consider $\mathbf{V}_I$ as the velocity field of a translating sphere with an arbitrary velocity given by $u_I\hat{\mathbf{z}}$. This translating sphere is subjected to no slip boundary condition on its surface. On the surface of the sphere, we have $\mathbf{V}_I = u_I\hat{\mathbf{z}}$. As a very well known result, for this translating sphere, the hydrodynamic force has a simple form given by $\mathbf{F}_I = -6\pi u_I\hat{\mathbf{z}}$. For case II, we choose the velocity profile of our main problem, the problem of a propelling Janus particle with slip velocity. We consider the problem of this propelling Janus particle in the laboratory reference frame and put $\mathbf{V}_{II} = \mathbf{V}' + \mathbf{U}'$. The slip condition on the particle surface is given by

$$\mathbf{V}_{II}|_S = \mathbf{V}'_S + \mathbf{U}', \tag{24}$$

where $\mathbf{V}'_S$ is the slip velocity from Equation (22). One should note that the hydrodynamic problems of both cases, I and II, vanish at infinity. Streamlines of the above two cases are plotted in Figure 2.

After defining problems I and II, we can easily see that the left-hand-side of Equation (23) reads as

$$\int \mathbf{V}_I \cdot \boldsymbol{\sigma}_{II} \cdot \hat{\mathbf{n}}\, dS = u_I\hat{\mathbf{z}} \cdot \int \boldsymbol{\sigma}_{II} \cdot \hat{\mathbf{n}}\, dS = u_I\hat{\mathbf{z}} \cdot \mathbf{F}_{II} = 0. \tag{25}$$

The last result comes from the force free condition of a self-propelling Janus particle. Then from the right-hand-side of Equation (23), we have

$$\int \mathbf{V}'_S \cdot \boldsymbol{\sigma}_I \cdot \hat{\mathbf{n}}\, dS = -\mathbf{U}' \cdot \mathbf{F}_I = 6\pi u_I U', \tag{26}$$

where we have used the fact that the force exerted on the particle in our first problem is given by $\mathbf{F}_I = -6\pi u_I\hat{\mathbf{z}}$. Substituting Equation (22) in the above equation, we will have

$$U' = \frac{1}{3\pi u_I} \ln\left(\cosh\frac{\zeta_0}{4}\right) \oint \sin\theta\, \hat{\boldsymbol{\theta}} \cdot \boldsymbol{\sigma}_I \cdot \hat{\mathbf{n}} dS. \tag{27}$$

Noting that for a spherical particle, we have $\hat{\mathbf{n}} \cdot \boldsymbol{\sigma}_I = -\frac{3}{2}u_I\hat{\mathbf{z}}$, and the propulsion velocity can be obtained as

$$\mathbf{U}' = \frac{4}{3} \ln\left(\cosh\frac{\zeta_0}{4}\right) \hat{\mathbf{z}}. \tag{28}$$

In Figure 3, we have plotted the ionic density profile and the streamlines of the resulting fluid flow around the self-propelled Janus particle. Asymmetric distribution of the ions around the Janus particle emerges from the asymmetric surface activity given on the surface of motor. Such an asymmetry, when combines with the slip velocity condition given in the macro-scale description, provides an essential physical element for producing a finite self-propulsion. After returning the physical dimensions, the speed of the Janus particle is given by

$$U = \frac{4}{3}\frac{\varepsilon_r (k_B T/e)^2}{\eta\, a}\frac{\dot{Q}a}{\mathcal{D}n_\infty} \ln\left(\cosh\frac{e\zeta_0}{4k_B T}\right). \tag{29}$$

The Janus particle moves in a direction that is preferred by the asymmetry of the surface reactions. Most important features of the above result can be summarized as follows. As one can see from the above result, both electric effect of Janus particle,

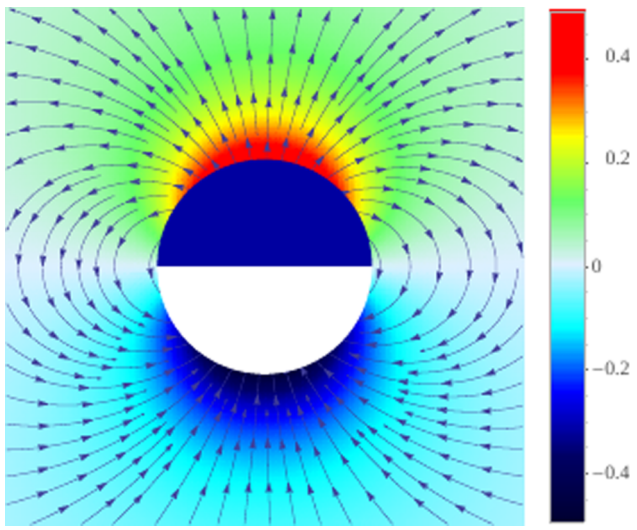

FIG. 3. Ionic density profile and fluid velocity streamlines of an electrokinetic self-propelled Janus particle. Asymmetric distribution of ions and slip velocity on the surface are essential elements that cause the Janus particle to move.

which is given by its surface potential ζ_0, and the strength of thermal fluctuations k_BT have dominant influence on the functionality of a single motor. In our model, n_∞ is constant and the flux of ions on the surface of motor $\dot{Q}$ plays the role of fuel for the motor, and increasing $\dot{Q}$ will increase the velocity of motor.

In the case of small Peclet number and for large temperature $k_BT \gg e\zeta_0$, the case that we are interested in a typical system, the swimming speed can be approximated as $U \sim (\pi/4)\varepsilon_r \dot{Q}\zeta_0^2 a_{\text{ion}} n_\infty^{-1}(k_BT)^{-1}$, where we have used the relations $\mathcal{D} = k_BT/\xi^{\text{ion}}$ and $\xi^{\text{ion}} = 6\pi\eta a_{\text{ion}}$ with the size of ionic molecules given by a_{ion}. As one can see, the thermal fluctuations have negative influence on the functionality of Janus motor. For a typical case with $\varepsilon_r = 80\epsilon_0$, $\dot{Q} = 10^7\ \mu\text{m}^{-2}\text{s}^{-1}$, $a_{\text{ion}} = 1$ nm, and $\zeta_0 = 0.01$ V, we arrive at a speed like $U \sim 1\ \mu\text{m s}^{-1}$. Such speed is completely reasonable to have a functional motor at the scale of micrometer.

After calculating the propulsion velocity, we can investigate the velocity field due to the self-propulsion of this single motor. The above approach works only for evaluating the particle speed. In order to obtain the velocity field, we should solve the Stokes equation with proper boundary conditions. A direct solution to the hydrodynamic equations, presented in Appendix A, reveals that the velocity field of a self-propelled Janus particle in the laboratory frame reads as

$$\mathbf{V}' = \frac{1}{2}\frac{1}{r^3}U'\left(2\cos\theta\ \hat{\mathbf{r}} + \sin\theta\ \hat{\theta}\right) = -\frac{1}{2}\frac{1}{r^3}\mathbf{U}'\cdot(\mathbb{I} - 3\hat{\mathbf{r}}\hat{\mathbf{r}}). \quad (30)$$

One should note that the above velocity field resembles the velocity field due to a dipole of sink and source of potential flow. As a result of the force free condition, we had this expectation from the beginning that in a multipole expansion of the velocity field, the source dipole should have the dominant effect.

VI. TWO INTERACTING JANUS PARTICLES

As shown in Figure 4, let us consider two spherically symmetric Janus particles with radii a_1 and a_2. These two particles are separated by a center to center vector denoted by $\mathbf{D}$. The position of a general point in space with respect to each motor is given by $\mathbf{r}_{1(2)}$, respectively. Intrinsic propulsion velocities of Janus particles point along the directions given by $\hat{\mathbf{t}}_{1(2)}$. In reference frames that are locally connected to each sphere, the polar angles are measured with respect to $\hat{\mathbf{t}}_{1,2}$ and are denoted by $\theta_{1,2}$ and $\varphi_{1,2}$. The surface activity of the Janus

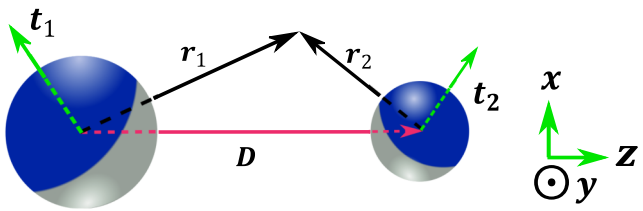

FIG. 4. Geometry of two spherical self-propelled Janus particles that are located in distance $\mathbf{D}$.

particles is given by

$$\hat{\mathbf{n}}_i \cdot \mathbf{j}_\pm(\mathbf{r}_i = a_i\hat{\mathbf{n}}_i) = \dot{Q}_i\cos\theta_i, \quad i = 1,2,$$

where $\hat{\mathbf{n}}_1$ and $\hat{\mathbf{n}}_2$ represent the unit vectors that are normal to the spheres and the ionic production rates at the surfaces of motors are denoted by $\dot{Q}_1$ and $\dot{Q}_2$. As a result of the calculation given in Sec. V, the intrinsic propulsion speed of motors, which are the speed of isolated motors, is given by Equation (28). We want to calculate the influences of a Janus particle on the speed of a nearby Janus particle.

At the limit of very small Debye layer, the case that we are interested here, the electric effects of particles are screened and the direct electrostatic interaction between the particles can be neglected. In this case, the electro-hydrodynamic forces should be considered.

Neglecting the direct electrostatic interaction between particles, two types of effects can mediate the electro-hydrodynamic forces. Both the direct hydrodynamic interaction between moving particles immersed in the fluid medium and the change of fluid pattern due to the rearrangement of ionic species which are subjected to instantaneous boundary condition on both particles will eventually lead to coupling between Janus particles. For simplicity, we call the former case by *direct* and denote the latter case by *indirect* contributions. The direct (indirect) interaction is due to the instantaneous appearance of particle positions in the boundary conditions of hydrodynamic (electrostatic) equations.

It is very important to note that both kinds of the above interactions are of hydrodynamics in nature and it is the fluid medium that mediates both types of the interactions. As an approximation, we assume that these two contributions are additive. The validity of this approximation is guaranteed for very far separated particles and we will clarify it in more detail in Sections VI A and VI B.

Denoting the overall translational and rotational velocities of each particle by $\mathbf{U}_i$ and Ω_i, we can write them as

$$\begin{aligned}\mathbf{U}_i &= \mathbf{U}_i^0 + \mathbf{U}_i^{\text{dir}} + \mathbf{U}_i^{\text{ind}},\\ \boldsymbol{\Omega}_i &= \boldsymbol{\Omega}_i^0 + \boldsymbol{\Omega}_i^{\text{dir}} + \boldsymbol{\Omega}_i^{\text{ind}},\end{aligned} \quad (31)$$

where the intrinsic translational and rotational propulsion velocities of the ith Janus particle are given by

$$\mathbf{U}_i^0 = \frac{4}{3}\dot{Q}_i \ln\left(\cosh\frac{\zeta_i}{4}\right)\hat{\mathbf{t}}_i, \quad \boldsymbol{\Omega}_i^0 = 0. \quad (32)$$

From here, we use the radius of the first sphere a_1 for making dimensionless lengths. This means that our results will depend on a new dimensionless number $e = (a_2/a_1)$.

We aim to calculate the direct and indirect contributions. As described before, the coupling between two particles arises from the boundary conditions that take into account the positions of two particles. The ionic concentration field satisfies the Poisson equation and it is subjected to boundary conditions on the outer part of the Debye layer of both Janus particles. In the limit of thin Debye layer with $\delta \to 0$, the Poisson equation simplifies to $\nabla^2 N = 0$, where $N(\mathbf{r}_1, \mathbf{r}_2)$ shows the ionic concentration outside the Debye layer (effective properties of bulk). The ionic concentration satisfies the

following boundary conditions:

$$\frac{\partial N}{\partial r_i} = -\dot{Q}_i \cos\theta_i, \qquad \mathbf{r}_i = \hat{\mathbf{n}}_i, \quad i = 1,2. \tag{33}$$

In addition to the above boundary conditions, the velocity field also should satisfy the Dukhin-Derjaguin slip velocity on the outer surface of Debye layer of each particle. The hydrodynamic boundary conditions read[51]

$$\mathbf{V}_{S_i} = -4 \ln\left(\cosh\frac{\zeta_{0_i}}{4}\right) \nabla_{S_i} N, \quad \mathbf{r}_i = \hat{\mathbf{n}}_i, \ \ i = 1,2, \tag{34}$$

where the tangential gradient operator is denoted by ∇_{S_i}.

Simultaneous application of two boundary conditions given by Equation (33) and Equation (34) is the main difficulty that makes it impossible to present a full analytic solution. In the limit of very far motors, $D \gg 1, e \sim 1$, we can proceed with a perturbation method. We first assume that the motors are hydrodynamically uncoupled and assume that the coupling is only due to the boundary condition on the ionic concentration. This will give us the indirect contribution. Then to obtain an approximation for the direct hydrodynamic contribution, we assume that the motors are decoupled with respect to ionic boundary conditions and investigate the hydrodynamic boundary conditions separately. This scheme will provide us a systematic way to expand the interaction in powers of $1/D$.

In the following, we first calculate the indirect contribution and then the direct hydrodynamic contribution is also calculated.

A. Indirect contribution

To obtain the indirect contribution, we should take into account the boundary condition on concentration field that is given by Equation (33). For very far particles ($D \gg 1$), we denote the concentration profiles for isolated particles by N_1^0 and N_2^0. In this case, we can write the real concentration field that obeys the full boundary conditions as

$$N = N_1^0 + N_2^0 + \Delta N, \tag{35}$$

where the deviations from isolated particle solution are denoted by ΔN. As have been calculated in Secs. I–V, the concentration profiles for isolated particles are given by

$$N_1^0 = \frac{\dot{Q}_1}{2r_1^2}\cos\theta_1, \quad N_2^0 = \frac{e^3\dot{Q}_2}{2r_2^2}\cos\theta_2. \tag{36}$$

Writing the deviation from single particle profile as

$$\Delta N = \sum_{\alpha=1}^{\infty} (N_1^\alpha + N_2^\alpha), \tag{37}$$

we can easily see that the new fields satisfy the Laplace equation as $\nabla^2 N_i^\alpha = 0$ with the boundary conditions given by

$$\frac{\partial N_i^\alpha}{\partial n} = -\frac{\partial N_j^{\alpha-1}}{\partial n}, \qquad \mathbf{r}_i = \hat{\mathbf{n}}_i, \quad i,j = 1,2. \tag{38}$$

Such hierarchical description of the effects of motors allows us to develop a systematic expansion in powers of $1/D$.

At the leading order of calculations, we can proceed by considering the zero order term. Having in hand the zero order concentration profile, we can use Equation (34) and evaluate the slip velocities on the surface of each motor. Performing such calculations, we can arrive at the following relations for the slip velocities. On the surface of first Janus particle, and in the laboratory reference frame, the velocity reads as

$$\begin{aligned}\mathbf{V}_{S_1}^{\text{ind}} = &-\frac{3}{2}\mathbf{U}_1^0 \cdot (\mathbb{I} - \hat{\mathbf{r}}_1\hat{\mathbf{r}}_1) - \frac{3}{2}\frac{e^3}{D^3}\,\mathbf{U}_2^0 \cdot \left(\mathbb{I} - 3\hat{\mathbf{D}}\hat{\mathbf{D}}\right) \cdot (\mathbb{I} - \hat{\mathbf{r}}_1\hat{\mathbf{r}}_1) \\ &+ \frac{9}{2}\frac{e^3}{D^4}\,\mathbf{U}_2^0 \cdot \left(-2\mathbb{I} + 5\hat{\mathbf{D}}\hat{\mathbf{D}}\right) \cdot \hat{\mathbf{r}}_1\hat{\mathbf{D}} \cdot (\mathbb{I} - \hat{\mathbf{r}}_1\hat{\mathbf{r}}_1) \\ &- \frac{9}{2}\frac{e^3}{D^4}\,\hat{\mathbf{r}}_1 \times (\mathbf{U}_2^0 \times \hat{\mathbf{D}}),\end{aligned} \tag{39}$$

and on the surface of second Janus particle, the slip velocity reads as

$$\begin{aligned}\mathbf{V}_{S_2}^{\text{ind}} = &-\frac{3}{2}\frac{1}{e^3}\,\mathbf{U}_2^0 \cdot (\mathbb{I} - \hat{\mathbf{r}}_2\hat{\mathbf{r}}_2) \\ &- \frac{3}{2}\frac{1}{D^3}\,\mathbf{U}_1^0 \cdot \left(\mathbb{I} - 3\hat{\mathbf{D}}\hat{\mathbf{D}}\right) \cdot (\mathbb{I} - \hat{\mathbf{r}}_2\hat{\mathbf{r}}_2) \\ &- \frac{9}{2}\frac{e}{D^4}\,\mathbf{U}_1^0 \cdot \left(-2\mathbb{I} + 5\hat{\mathbf{D}}\hat{\mathbf{D}}\right) \cdot \hat{\mathbf{r}}_2\hat{\mathbf{D}} \cdot (\mathbb{I} - \hat{\mathbf{r}}_2\hat{\mathbf{r}}_2) \\ &+ \frac{9}{2}\frac{e}{D^4}\,\hat{\mathbf{r}}_2 \times (\mathbf{U}_1^0 \times \hat{\mathbf{D}}).\end{aligned} \tag{40}$$

As one can see, the slip velocity on each particle has two contributions. As an example, and for the first particle, these two contributions are the term that is proportional to $\mathbf{U}_1^0$ and the terms that are proportional to $\mathbf{U}_2^0$. The first term denotes the intrinsic asymmetry of the particle while the other parts are due to the asymmetry of the second Janus particle.

As a result of the above surface slip velocities, the velocity field in the medium deviates from its value for the isolated Janus particles. Now to obtain the full changes in the velocity field, we need to apply the full hydrodynamic boundary conditions on both particles. Here, we want to neglect such complexities and simply assume that the velocity profile is still due to the isolated Janus particles but with modified slip velocities given by the above relations. This is the core of our direct-indirect separation of the effects and what we obtain with this assumption contains the indirect contribution. In Sec. VI B, we will again come back to this point and take into account the effects that we neglected here.

We write the fluid velocity field in the laboratory frame as

$$\mathbf{V}^{\text{ind}} = \mathbf{V}_1^{\text{ind}} + \mathbf{V}_2^{\text{ind}}, \tag{41}$$

where the partial flows due to each Janus particle can be written as

$$\begin{aligned}\mathbf{V}_1^{\text{ind}} &= -\frac{1}{2}\frac{1}{r_1^3}\left(\mathbf{U}_1^0 + \mathbf{U}_1^{\text{ind}}\right) \cdot (\mathbb{I} - 3\hat{\mathbf{r}}_1\hat{\mathbf{r}}_1) + O(\frac{1}{r_1})^4, \\ \mathbf{V}_2^{\text{ind}} &= -\frac{1}{2}\frac{e^3}{r_2^3}\left(\mathbf{U}_2^0 + \mathbf{U}_2^{\text{ind}}\right) \cdot (\mathbb{I} - 3\hat{\mathbf{r}}_2\hat{\mathbf{r}}_2) + O(\frac{1}{r_2})^4,\end{aligned} \tag{42}$$

where the velocity contributions that the particles achieved from indirect interaction are denoted by $\mathbf{U}_i^{\text{ind}}$ and $\mathbf{\Omega}_i^{\text{ind}}$. The above relations are essentially the velocity profiles of isolated Janus particles given in Equation (30), but with modified swimming velocities.

Two important conditions of zero total force and zero total torque are essential points that we should apply to the equations for obtaining $\mathbf{U}_i^{\text{ind}}$ and $\mathbf{\Omega}_i^{\text{ind}}$. Similar to the case of a single Janus particle, we can use the Lorentz reciprocal theorem and extract the required results. The details of such calculations are collected in Appendix B. For the first particle, the final results read

$$\begin{aligned}\mathbf{U}_1^{\text{ind}} &= \frac{e^3}{D^3} U_2^0\, \hat{\mathbf{t}}_2 \cdot \left(\mathbb{I} - 3\hat{\mathbf{D}}\hat{\mathbf{D}}\right),\\ \mathbf{\Omega}_1^{\text{ind}} &= -\frac{9}{2}\frac{e^3}{D^4} U_2^0 \left(\hat{\mathbf{t}}_2 \times \hat{\mathbf{D}}\right),\end{aligned} \tag{43}$$

and for the second particle, we will have

$$\begin{aligned}\mathbf{U}_2^{\text{ind}} &= \frac{1}{D^3} U_1^0\, \hat{\mathbf{t}}_1 \cdot \left(\mathbb{I} - 3\hat{\mathbf{D}}\hat{\mathbf{D}}\right),\\ \mathbf{\Omega}_2^{\text{ind}} &= \frac{9}{2}\frac{e}{D^4} U_1^0 \left(\hat{\mathbf{t}}_1 \times \hat{\mathbf{D}}\right).\end{aligned} \tag{44}$$

The above results present the zero order indirect contributions, regarding the perturbation expansion introduced in Equation (35). As one can see, the results for translation velocity decay like $(1/D)^3$. To see the effects of the next order terms, we need to solve the Laplace equation for N_i^1 with proper boundary condition given by Equation (38). As the boundary condition decays like $(1/D)^2$ and the governing equation is also linear, we will expect such a similar decay for N_i^1. Now for calculating the effects of such first order term in the velocities, we should repeat the same procedure as described for zero order term. Continuing the calculations, we will eventually receive at a velocity correction for Janus particles that decay like $(1/D)^3 \times (1/D)^2$. At the next part, we will show that the direct hydrodynamic contribution gives corrections that are more effective than these corrections. So we will ignore the higher order corrections due to the concentration profile and keep only the zero order contribution.

B. Direct hydrodynamic contribution

In Sec. VI A, we have neglected the complexities associated with simultaneous applications of the slip velocity condition on both particles. We have simply assumed that the velocity profile corresponds to the isolated Janus particles but with modified slip velocities. Here, we want to go beyond this simplification and obtain the corrections associated to such complexities. To achieve the overall velocity field $\mathbf{V}$, associated to the complete problem that takes into account both direct and indirect interactions, a Stokes equation with the following boundary conditions on the surface of Janus particles should be solved:

$$\begin{aligned}\mathbf{V}|_{S_1} &= \mathbf{U}_1^0 + \mathbf{U}_1^{\text{ind}} + \mathbf{\Omega}_1^{\text{ind}} \times \mathbf{r}_1 + \mathbf{U}_1^{\text{dir}} + \mathbf{\Omega}_1^{\text{dir}} \times \mathbf{r}_1 + \mathbf{V}_{S_1}^{\text{ind}},\\ \mathbf{V}|_{S_2} &= \mathbf{U}_2^0 + \mathbf{U}_2^{\text{ind}} + \mathbf{\Omega}_2^{\text{ind}} \times (\mathbf{r}_1 - \mathbf{D})\\ &\quad + \mathbf{U}_2^{\text{dir}} + \mathbf{\Omega}_2^{\text{dir}} \times (\mathbf{r}_1 - \mathbf{D}) + \mathbf{V}_{S_2}^{\text{ind}},\\ \mathbf{V}|_{\infty} &= 0,\end{aligned} \tag{45}$$

where we have assumed that as a result of hydrodynamic interaction between the particles, each Janus particle achieves an additional change in its velocities given by $\mathbf{U}_i^{\text{dir}}$ and $\mathbf{\Omega}_i^{\text{dir}}$. Again a proper application of Lorentz reciprocal theorem will help us to extract the required velocities. The details of calculations are presented in Appendix C, and here we write the final results. For the first Janus particle and up to the order $O(1/D)^6$, we will have

$$\begin{aligned}\mathbf{U}_1^{\text{dir}} = &-\frac{1}{2}\frac{e^3}{D^3} U_2^0\, \hat{\mathbf{t}}_2 \cdot \left(\mathbb{I} - 3\hat{\mathbf{D}}\hat{\mathbf{D}}\right)\\ &-\frac{1}{2}\frac{e^3}{D^6} U_1^0\, \hat{\mathbf{t}}_1 \cdot \left(\mathbb{I} - 3\hat{\mathbf{D}}\hat{\mathbf{D}}\right) \cdot \left(\mathbb{I} - 3\hat{\mathbf{D}}\hat{\mathbf{D}}\right),\end{aligned} \tag{46}$$

the first term that is proportional to U_2^0 is the velocity field produced by the second Janus particle and calculated at the position of first Janus particle. This is a result that we expected to see from the Faxen theorem for a colloidal particle immersed in external velocity field. Calculations show that the dominant part of the rotational velocity induced by direct interaction will behave like $(1/D)^9$, and we neglect it here. Similar expression can be obtained for the second Janus particle that reads as

$$\begin{aligned}\mathbf{U}_2^{\text{dir}} = &-\frac{1}{2}\frac{1}{D^3} U_1^0\, \hat{\mathbf{t}}_1 \cdot \left(\mathbb{I} - 3\hat{\mathbf{D}}\hat{\mathbf{D}}\right)\\ &-\frac{1}{2}\frac{1}{D^6} U_2^0\, \hat{\mathbf{t}}_2 \cdot \left(\mathbb{I} - 3\hat{\mathbf{D}}\hat{\mathbf{D}}\right) \cdot \left(\mathbb{I} - 3\hat{\mathbf{D}}\hat{\mathbf{D}}\right).\end{aligned} \tag{47}$$

Very interestingly, the dominant part of both direct and indirect contributions behaves similarly for $D \gg 1$. Therefore, the dominant part of the total translational and rotational velocity of the first Janus particle is given by

$$\begin{aligned}\mathbf{U}_1 &= \mathbf{U}_1^0 + \frac{1}{2}\frac{e^3}{D^3} U_2^0\, \hat{\mathbf{t}}_2 \cdot \left(\mathbb{I} - 3\hat{\mathbf{D}}\hat{\mathbf{D}}\right),\\ \mathbf{\Omega}_1 &= -\frac{9}{2}\frac{e^3}{D^4} U_2^0 \left(\hat{\mathbf{t}}_2 \times \hat{\mathbf{D}}\right).\end{aligned} \tag{48}$$

As a result of symmetry, the corresponding velocities of the second Janus particle can be written as

$$\begin{aligned}\mathbf{U}_2 &= \mathbf{U}_2^0 + \frac{1}{2}\frac{1}{D^3} U_1^0\, \hat{\mathbf{t}}_1 \cdot \left(\mathbb{I} - 3\hat{\mathbf{D}}\hat{\mathbf{D}}\right),\\ \mathbf{\Omega}_2 &= \frac{9}{2}\frac{e}{D^4} U_1^0 \left(\hat{\mathbf{t}}_1 \times \hat{\mathbf{D}}\right).\end{aligned} \tag{49}$$

In the next part, we show how such interactions will modify the trajectories of Janus particles.

VII. RESULTS AND DISCUSSION

At the limit of $\mathcal{D}a \ll 1$, $\mathcal{R}e \ll 1$, $\mathcal{P}e \ll 1$, and $\kappa a \gg 1$, we have considered the physics of interacting Janus motors. As a result of small Reynolds number, we have neglected the inertia effects in the motion of fluid. Small Damkohler number ensures us that the surface flux of the ions does not violate the equilibrium conditions of the system. We have shown that as a result of coupling between hydrodynamic and electrostatic effects, a long-range interaction between particles has been mediated. For a very thin Debye layer $\kappa a \gg 1$ and $a \ll D$, the electrostatic effects of Janus particles are screened and we have neglected the electric interaction of the Janus particles. In this case, all the interactions between particles have hydrodynamical origin that is long range. Such long range interaction affects the translational velocity of each motor, and it also introduces a rotational velocity for motors. For very far Janus particles, the leading order of translational speed scales as $O\left([1/D]^3\right)$ and angular velocity

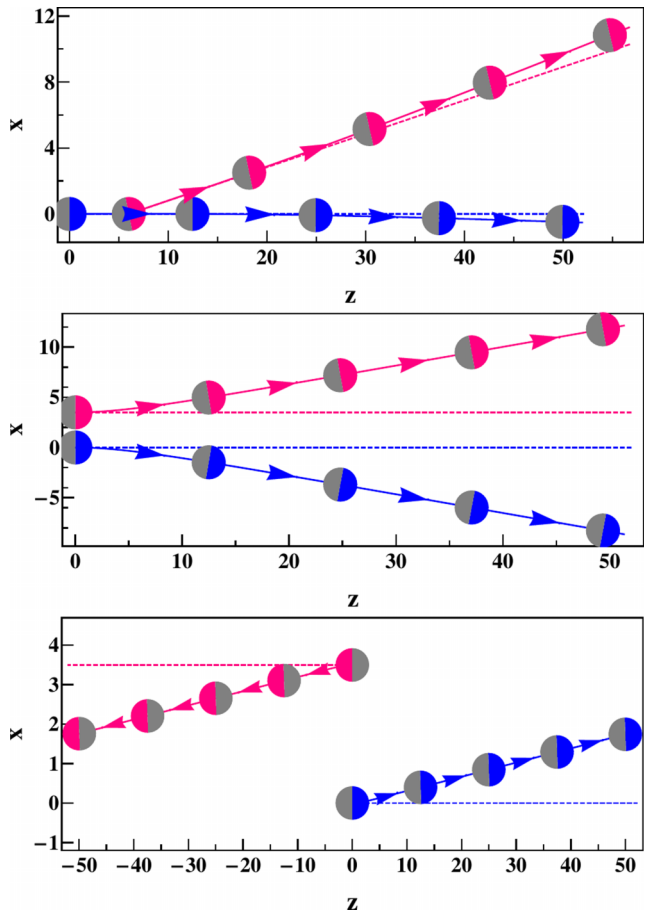

FIG. 5. Trajectories of two interacting Janus particles are shown for different initial states of the motors. In all figures, the intrinsic speed of the motors is assumed to be similar. As one can see, for the case of two parallel motors, the interaction tends to repel the Janus particles.

scales as $O\left([1/D]^4\right)$. The interaction modifies the trajectories of self-propelling Janus particles. To have a qualitative feeling of the interaction, some typical examples of the trajectories are presented in Figure 5. As one can distinguish from figures, the overall effect of the interaction depends on the initial states of two Janus particles. In all trajectories, the dashed-line corresponds to the trajectory of an isolated Janus particle. For the cases where the particles move in same directions (the first two trajectories shown in figure), the interaction has a repulsive signature. But for a case where the particles move in anti-parallel directions (the third trajectory shown in Figure 5), the interaction tends to decrease the relative speed of two particles. Such behavior is reminiscent of the generic picture of hydrodynamic interactions between particles. A particle moving in a fluid medium with very low Reynolds number produces a flow field that instantaneously propagates to the position of a second particle. The propagated flow tends to increase the relative velocity of two particles. This eventually will show an effective repulsion between particles. We have used the dominant part of the interactions but please note that by using the method that we have developed in this paper, we are able to systematically consider all of the orders of perturbation terms.

Along this work, we are currently working on the dynamics of a collection of active Janus particles. It is a known fact that hydrodynamic interaction near a rough wall will introduce nontrivial effects;[53] in this case, we are also analyzing the motion of a single Janus motor near a wall with surface roughness.

APPENDIX A: VELOCITY FIELD DUE TO A SINGLE ACTIVE JANUS PARTICLE

In this appendix, we present the detail of the calculations for the velocity field produced by a moving single Janus motor. Along this task, we should solve the Stokes equation, with boundary conditions given as follows:

$$\begin{aligned}\mathbf{V}'|_{\infty} &= -U'\hat{\mathbf{z}} = -U'\cos\theta\,\hat{\mathbf{r}} + U'\sin\theta\,\hat{\boldsymbol{\theta}},\\ \mathbf{V}'|_{r=1} &= -4\ln\left(\cosh\frac{\zeta_0}{4}\right)\nabla_S N'|_{r=1}\\ &= \frac{3}{2}U'\sin\theta\,\hat{\theta}.\end{aligned}$$

To proceed, we eliminate the pressure field from the Stokes equation by evaluating the curl of this equation. This will give us the following equation:

$$\nabla\times(\nabla^2\mathbf{V}') = \nabla^2(\nabla\times\mathbf{V}') = 0.$$

In terms of stream function $H(r,\theta)$, the velocity field can be written as

$$\mathbf{V}' = \frac{1}{r\sin\theta}\frac{\partial H}{\partial r}\,\hat{\boldsymbol{\theta}} - \frac{1}{r^2\sin\theta}\frac{\partial H}{\partial\theta}\,\hat{\mathbf{r}},$$

where the incompressibility condition $\nabla\cdot\mathbf{V}' = 0$ is assumed. According to the boundary condition at infinity, one can suggest a solution for H as

$$H(r,\theta) = f(r)\sin^2\theta.$$

Using the above ansatz, the curl of velocity field reads as

$$\begin{aligned}\nabla\times\mathbf{V}' &= \left(\frac{1}{r}\frac{d^2f}{dr^2} - \frac{2}{r^3}f\right)\sin\theta\,\hat{\boldsymbol{\varphi}}\\ &= A(r)\sin\theta\,\hat{\boldsymbol{\varphi}},\end{aligned}$$

where $A(r) = \frac{1}{r}\frac{d^2f}{dr^2} - \frac{2}{r^3}f$. Now we can write

$$\nabla^2(\nabla\times\mathbf{V}') = \hat{\boldsymbol{\varphi}}\,\sin\theta\left[\frac{d^2A}{dr^2} + \frac{2}{r}\frac{dA}{dr} - \frac{2A}{r^2}\right] = 0.$$

So we have following equation for $A(r)$:

$$\frac{d^2A}{dr^2} + \frac{2}{r}\frac{dA}{dr} - \frac{2A}{r^2} = 0,$$

and its solution is

$$A = B_1'r + \frac{B_2'}{r^2},$$

where B_1', B_2' are integration constants. Function f satisfies the following differential equation:

$$\frac{d^2f}{dr^2} - \frac{2}{r^2}f - B_1'r^2 + \frac{B_2'}{r} = 0,$$

which has a general solution like

$$f = B_1r^4 + B_2r + C_1r^2 + \frac{C_2}{r}.$$

Collecting all the above results, we can write the fluid velocity field as

$$\mathbf{V}' = -\frac{2}{r^2}\left(B_1 r^4 + B_2 r + C_1 r^2 + \frac{C_2}{r}\right)\cos\theta\,\hat{\mathbf{r}} + \frac{1}{r}\left(4B_1 r^3 + B_2 + 2C_1 r - \frac{C_2}{r^2}\right)\sin\theta\,\hat{\boldsymbol{\theta}},$$

where B_1, B_2, C_1, and C_2 are constants that can be easily determined by applying the boundary conditions. Finally, the fluid velocity field due to a moving Janus particle in a co-moving reference frame reads as

$$\mathbf{V}' = -U'\,\hat{\mathbf{z}} + \frac{1}{2}\frac{U'}{r^3}\left(2\cos\theta\,\hat{\mathbf{r}} + \sin\theta\,\hat{\boldsymbol{\theta}}\right) = -\mathbf{U}' - \frac{1}{2}\mathbf{U}'\cdot\left(\frac{\mathbb{I} - 3\hat{\mathbf{r}}\hat{\mathbf{r}}}{r^3}\right).$$

APPENDIX B: INDIRECT CONTRIBUTION TO THE INTERACTION

In this appendix, we present the calculations that give the indirect contribution to the interaction between two Janus particles. We just consider the contribution to the velocity of the first motor, then the symmetry arguments will help us to write the velocity change of the second motor as well. As in the case of a single Janus particle, we will benefit the Lorentz reciprocal theorem to extract the indirect contribution. To use the reciprocal theorem, we need to define the set of two hydrodynamic problems which share a common geometry but with different boundary conditions. Let us start with defining problem II, first. Case II corresponds to our main problem defined in Sec. VI A. We put $\mathbf{V}_{II} = \mathbf{V}^{\text{ind}}$ and it is subjected to the following boundary conditions:

$$\mathbf{V}_{II}|_{S_1} = \mathbf{U}_1^0 + \mathbf{U}_1^{\text{ind}} + \boldsymbol{\Omega}_1^{\text{ind}} \times \mathbf{r}_1 + \mathbf{V}_{S_1}^{\text{ind}},$$

where we would like to find $\mathbf{U}_1^{\text{ind}}$ and $\boldsymbol{\Omega}_1^{\text{ind}}$ and note that the calculations should be done in laboratory frame. Here $\mathbf{V}_{S_1}^{\text{ind}}$ is the slip velocity given by Equation (39), and $\mathbf{U}_1^0$ is the first particle velocity from Equation (32).

As we are looking for 6 unknown variables (the components of $\mathbf{U}_1^{\text{ind}}$ and $\boldsymbol{\Omega}_1^{\text{ind}}$), we can consider 6 different choices for problem I. To evaluate 3 components for $\mathbf{U}_1^{\text{ind}}$, we choose $\mathbf{V}_I$ as the velocity field of a translating particle with velocity u_I in the three major Cartesian directions, and in order to evaluate 3 components of $\boldsymbol{\Omega}_1^{\text{ind}}$, we choose the velocity field of a rotating particle with velocity ω_I in the three major directions. On the surface of the first particle, we have $\mathbf{V}_I|_{S_1} = \mathbf{u}_I + \boldsymbol{\omega}_I \times \mathbf{r}_1$, where

$$(\mathbf{u}_I, \boldsymbol{\omega}_I)_{j=1} = (u_I\hat{\mathbf{x}}, 0), \quad (\mathbf{u}_I, \boldsymbol{\omega}_I)_{j=4} = (0, \omega_I\hat{\mathbf{x}}),$$
$$(\mathbf{u}_I, \boldsymbol{\omega}_I)_{j=2} = (u_I\hat{\mathbf{y}}, 0), \quad (\mathbf{u}_I, \boldsymbol{\omega}_I)_{j=5} = (0, \omega_I\hat{\mathbf{y}}),$$
$$(\mathbf{u}_I, \boldsymbol{\omega}_I)_{j=3} = (u_I\hat{\mathbf{z}}, 0), \quad (\mathbf{u}_I, \boldsymbol{\omega}_I)_{j=6} = (0, \omega_I\hat{\mathbf{z}}),$$

where $j = 1, 2, 3$ denote the cases of translation along the directions $\hat{\mathbf{x}}, \hat{\mathbf{y}}$, and $\hat{\mathbf{z}}$, respectively, and $j = 4, 5, 6$ denote the corresponding cases for rotations along $\hat{\mathbf{x}}, \hat{\mathbf{y}}$, and $\hat{\mathbf{z}}$. Note that for all of the above 6 cases, on the surface of the second particle, we have $\mathbf{V}_I|_{S_2} = 0$. Substituting these choices into the left-hand-side of Equation (23), we will obtain

$$\int \mathbf{V}_I \cdot \boldsymbol{\sigma}_{II} \cdot \hat{\mathbf{n}}\, dS = \int_{S_1} (\mathbf{u}_I + \boldsymbol{\omega}_I \times \mathbf{r}_1) \cdot \boldsymbol{\sigma}_{II} \cdot \hat{\mathbf{n}}\, dS = \mathbf{u}_I \cdot \int_{S_1} \boldsymbol{\sigma}_{II} \cdot \hat{\mathbf{n}}\, dS + \boldsymbol{\omega}_I \cdot \int_{S_1} \mathbf{r}_1 \times \boldsymbol{\sigma}_{II} \cdot \hat{\mathbf{n}}\, dS = \mathbf{u}_I \cdot \mathbf{F}_1 + \boldsymbol{\omega}_I \cdot \mathbf{L}_1 = 0,$$

where $\mathbf{F}_{II}$ and $\mathbf{L}_{II}$ are the force and torque exerted on the particle 1 and are equal to zero. Then from the right-hand-side of Equation (23), we have

$$\left(\mathbf{U}_1^0 + \mathbf{U}_1^{\text{ind}}\right) \cdot \int_{S_1} \boldsymbol{\sigma}_I \cdot \hat{\mathbf{n}}\, dS + \boldsymbol{\Omega}_1^{\text{ind}} \cdot \int_{S_1} \mathbf{r}_1 \times \boldsymbol{\sigma}_I \cdot \hat{\mathbf{n}}\, dS + \int_{S_1} \mathbf{V}_{S_1}^{\text{ind}} \cdot \boldsymbol{\sigma}_I \cdot \hat{\mathbf{n}}\, dS = 0,$$

where $\mathbf{F}_I = \int_{S_1} \boldsymbol{\sigma}_I \cdot \hat{\mathbf{n}}\, dS$ and $\mathbf{L}_I = \int_{S_1} \mathbf{r}_1 \times \boldsymbol{\sigma}_I \cdot \hat{\mathbf{n}}\, dS$ are the force and torque exerted on the particle in problem I. Now for the first three problems ($j = 1, 2, 3$) where

$$\boldsymbol{\omega}_I = 0, \quad \mathbf{F}_I = -6\pi\mathbf{u}_I, \quad \mathbf{L}_I = 0, \quad \boldsymbol{\sigma}_I \cdot \hat{\mathbf{n}} = -\frac{3}{2}\mathbf{u}_I,$$

we have

$$-6\pi\left(\mathbf{U}_1^0 + \mathbf{U}_1^{\text{ind}}\right) \cdot \mathbf{u}_I + \int_{S_1} \mathbf{V}_{S_1}^{\text{ind}} \cdot \boldsymbol{\sigma}_I \cdot \hat{\mathbf{n}}\, dS = 0$$

and

$$\int_{S_1} \mathbf{V}_{S_1}^{\text{ind}} \cdot \boldsymbol{\sigma}_I \cdot \hat{\mathbf{n}}\, dS = -\frac{3}{2}\left(\int_{S_1} \mathbf{V}_{S_1}^{\text{ind}} dS\right) \cdot \mathbf{u}_I = -6\pi\mathbf{U}_1^0 \cdot \mathbf{u}_I - 6\pi\frac{a_2^3}{D^3}\mathbf{U}_2^0 \cdot \left(\mathbb{I} - 3\hat{\mathbf{D}}\hat{\mathbf{D}}\right) \cdot \mathbf{u}_I.$$

Thus, the desired velocity due to indirect interaction is obtained as follows:

$$\mathbf{U}_1^{\text{ind}} = \frac{e^3}{D^3} U_2^0\, \hat{\mathbf{t}}_2 \cdot \left(\mathbb{I} - 3\hat{\mathbf{D}}\hat{\mathbf{D}}\right).$$

With similar calculations for the other three problems ($j = 3, 4, 5$), we can find $\boldsymbol{\Omega}_1^{\text{ind}}$ as follows:

$$\boldsymbol{\Omega}_1^{\text{ind}} = -\frac{9}{2}\frac{e^3}{D^4} U_2^0 \left(\hat{\mathbf{t}}_2 \times \hat{\mathbf{D}}\right).$$

Similarly, for the second particle, we have

$$\mathbf{U}_2^{\text{ind}} = \frac{1}{D^3} U_1^0\, \hat{\mathbf{t}}_1 \cdot \left(\mathbb{I} - 3\hat{\mathbf{D}}\hat{\mathbf{D}}\right),$$
$$\boldsymbol{\Omega}_2^{\text{ind}} = \frac{9}{2}\frac{e}{D^4} U_1^0 \left(\hat{\mathbf{t}}_1 \times \hat{\mathbf{D}}\right).$$

APPENDIX C: DIRECT CONTRIBUTION TO THE INTERACTION

We have denoted the overall velocity field of the full problem of interacting Janus particles by $\mathbf{V}$, and it is constrained to the boundary conditions given by Equation (45). Here we apply the reciprocal theorem to extract the direct hydrodynamic interaction between Janus particles. In the absence of direct hydrodynamic interaction, we denote the velocity field produced by the second Janus particle as $\mathbf{u}_\infty(\mathbf{r})$. The first Janus particle is floated in this field and

it is subjected to the proper boundary conditions. To use the reciprocal theorem, we consider the case of problem II as $\mathbf{V}_{II} = \mathbf{V} - \mathbf{u}_\infty(\mathbf{r})$ and it is subjected to the following conditions:

$$\begin{aligned}\mathbf{V}_{II}|_{S_1} &= \mathbf{U}_1^0 + \mathbf{U}_1^{\text{ind}} + \boldsymbol{\Omega}_1^{\text{ind}} \times \mathbf{r}_1 + \mathbf{V}_{S_1}^{\text{ind}} \\ &\quad + \mathbf{U}_1^{\text{dir}} + \boldsymbol{\Omega}_1^{\text{dir}} \times \mathbf{r}_1 - \mathbf{u}_\infty(0), \\ \mathbf{V}_{II}|_{S_2} &= 0,\end{aligned}$$

where $\mathbf{u}_\infty(0)$ is the flow field due to the second particle given at the center of the first particle. $\mathbf{U}_1^{\text{ind}}$ and $\boldsymbol{\Omega}_1^{\text{ind}}$ are the first Janus particle velocities due to the indirect hydrodynamic interaction and $\mathbf{V}_{S_1}^{\text{ind}}$ is the slip condition that is given by Equation (39). Velocities $\mathbf{U}_1^{\text{dir}}$ and $\boldsymbol{\Omega}_1^{\text{dir}}$ are unknowns that we want to find. So we have six unknown components and we should apply Lorentz theorem six times, as we did in Appendix B. We consider the problem of case I, as a spherical particle which moves with constant translational and rotational velocities given by $\mathbf{u}_I$ and $\boldsymbol{\omega}_I$. This sphere is immersed in an external velocity field given by $\mathbf{u}_\infty(\mathbf{r})$ and it is subjected to no slip boundary condition. Therefore, in the laboratory reference frame, on the surface of Janus particles, we have $\mathbf{V}_I|_{S_1} = \mathbf{u}_I + \boldsymbol{\omega}_I \times \mathbf{r}_1 - \mathbf{u}_\infty(0)$ and $\mathbf{V}_I|_{S_2} = 0$. To evaluate the different components of unknown velocities, we will choose six different choices for $\mathbf{u}_I$ and $\boldsymbol{\omega}_I$ as have been chosen in Appendix B.

Substituting into Equation (23) then, simplifying the results, we will arrive at

$$\begin{aligned}&\left(\mathbf{U}_1^0 + \mathbf{U}_1^{\text{dir}} + \mathbf{U}_1^{\text{ind}}\right) \cdot \mathbf{F}_I + \left(\boldsymbol{\Omega}_1^{\text{dir}} + \boldsymbol{\Omega}_1^{\text{ind}}\right) \cdot \mathbf{L}_I \\ &\quad = \int_{S_1} \mathbf{u}_\infty \cdot \boldsymbol{\sigma}_I \cdot \hat{\mathbf{n}}\, dS - \int_{S_1} \mathbf{V}_{S_1}^{\text{ind}} \cdot \boldsymbol{\sigma}_I \cdot \hat{\mathbf{n}}\, dS.\end{aligned}$$

Now we consider the three problems $j = 1, 2, 3$ (the problems that have been defined in Appendix B). So the right-hand-side terms are calculated as

$$\begin{aligned}&\int_{S_1} \mathbf{u}_\infty \cdot \boldsymbol{\sigma}_{\text{I}} \cdot \hat{\mathbf{n}}\, dS \\ &\quad = -\frac{3}{2}\mathbf{u}_{\text{I}} \cdot \int_{S_1} \mathbf{u}_\infty\, dS \\ &\quad \approx -\frac{3}{2}\mathbf{u}_{\text{I}} \cdot 4\pi \left(\mathbf{u}_\infty(\mathbf{r}_1 = 0) + \frac{1}{6}\nabla^2 \mathbf{u}_\infty(\mathbf{r}_1 = 0)\right) \\ &\quad \approx -6\pi \mathbf{u}_{\text{I}} \cdot \left(-\frac{1}{2}\frac{e^3}{D^3}\left(\mathbf{U}_2^0 + \mathbf{U}_2^{\text{ind}}\right) \cdot (\mathbb{I} - 3\hat{\mathbf{D}}\hat{\mathbf{D}}) + O\left(\frac{1}{D^6}\right)\right)\end{aligned}$$

and

$$\begin{aligned}&\int \mathbf{V}_{S_1}^{\text{ind}} \cdot \boldsymbol{\sigma}_{\text{I}} \cdot \hat{\mathbf{n}}\, dS \\ &\quad = -\frac{9}{4}\left(\mathbf{U}_1^0 + \mathbf{U}_1^{\text{ind}}\right) \cdot \int_{S_1} (\hat{\mathbf{r}}\hat{\mathbf{r}} - \mathbb{I})\, d\cos\theta\, d\varphi \cdot \mathbf{u}_{\text{I}} \\ &\quad = 6\pi \left(\mathbf{U}_1^0 + \mathbf{U}_1^{\text{ind}}\right) \cdot \mathbf{u}_{\text{I}}.\end{aligned}$$

Now collecting the above results, we have

$$\begin{aligned}-6\pi\left(\mathbf{U}_1^0 + \mathbf{U}_1^{\text{dir}} + \mathbf{U}_1^{\text{ind}}\right) \cdot \mathbf{u}_{\text{I}} &= -6\pi \mathbf{U}_1^0 \cdot \mathbf{u}_{\text{I}} - 6\pi \mathbf{U}_1^{\text{ind}} \cdot \mathbf{u}_{\text{I}} \\ &\quad - 6\pi\left(-\frac{1}{2}\frac{e^3}{D^3}\left(\mathbf{U}_2^0 + \mathbf{U}_2^{\text{ind}}\right) \cdot (\mathbb{I} - 3\hat{\mathbf{D}}\hat{\mathbf{D}}) + O\left(\frac{1}{D^6}\right)\right) \cdot \mathbf{u}_{\text{I}}.\end{aligned}$$

The final result for $\mathbf{U}_1^{\text{dir}}$ can be written as

$$\begin{aligned}\mathbf{U}_1^{\text{dir}} &= -\frac{1}{2}\frac{e^3}{D^3}\mathbf{U}_2^0 \cdot (\mathbb{I} - 3\hat{\mathbf{D}}\hat{\mathbf{D}}) - \frac{1}{2}\frac{e^3}{D^3}\mathbf{U}_2^{\text{ind}} \cdot (\mathbb{I} - 3\hat{\mathbf{D}}\hat{\mathbf{D}}) \\ &\quad + O\left(\frac{1}{D^6}\right).\end{aligned}$$

Now for evaluating $\boldsymbol{\Omega}^{\text{dir}}$, we consider three problems given as $j = 4, 5, 6$ in Appendix B. For these cases, we have

$$\mathbf{u}_I = 0, \quad \mathbf{F}_I = 0, \quad \mathbf{L}_I = -8\pi\boldsymbol{\omega}_I, \quad \boldsymbol{\sigma}_I \cdot \hat{\mathbf{n}} = -3\,\boldsymbol{\omega}_I \times \hat{\mathbf{r}}_1.$$

So the right-hand-side terms of the reciprocal integral are calculated as

$$\begin{aligned}&\int_{S_1} \mathbf{u}_\infty \cdot \boldsymbol{\sigma}_{\text{I}} \cdot \hat{\mathbf{n}}\, dS \\ &\quad = -3\,\boldsymbol{\omega}_{\text{I}} \cdot \int_{S_1} \hat{\mathbf{r}} \times \mathbf{u}_\infty\, dS \\ &\quad \approx -3\,\boldsymbol{\omega}_{\text{I}} \cdot \int_{S_1} \hat{\mathbf{r}} \times \left(\mathbf{u}_\infty(\mathbf{r}_1 = 0) + \frac{4\pi}{3}\nabla \times \mathbf{u}_\infty(\mathbf{r}_1 = 0)\right) \\ &\quad \approx O\left(\frac{1}{D^9}\right)\end{aligned}$$

and

$$\begin{aligned}\int \mathbf{V}_{S_1}^{\text{ind}} \cdot \boldsymbol{\sigma}_{\text{I}} \cdot \hat{\mathbf{n}}\, dS &= -3\,\boldsymbol{\omega}_{\text{I}} \cdot \int_{S_1} \hat{\mathbf{r}} \times \mathbf{V}_{S_1}^{\text{ind}}\, d\cos\theta\, d\varphi \\ &= -36\pi\frac{e^3}{D^4}\left(\mathbf{U}_2^0 \times \hat{\mathbf{D}}\right) \cdot \boldsymbol{\omega}_{\text{I}}, \\ &= 8\pi\,\boldsymbol{\Omega}^{\text{ind}} \cdot \boldsymbol{\omega}_{\text{I}}.\end{aligned}$$

Substituting the above results into the reciprocal integral, we can see that

$$-8\pi\left(\boldsymbol{\Omega}^{\text{ind}} + \boldsymbol{\Omega}^{\text{dir}}\right) \cdot \boldsymbol{\omega}_{\text{I}} = -8\pi\,\boldsymbol{\Omega}^{\text{ind}} \cdot \boldsymbol{\omega}_{\text{I}} + O\left(\frac{1}{D^9}\right).$$

This shows that the rotational velocity has no direct contribution behaving stronger than a term like $(1/D)^9$.

[1]E. R. Kay, D. A. Leigh, and F. Zerbetto, "Synthetic molecular motors and mechanical machines," Angew. Chem., Int. Ed. **46**(1–2), 72–191 (2007).
[2]E. Lauga and T. R. Powers, "The hydrodynamics of swimming microorganisms," Rep. Prog. Phys. **72**(9), 096601 (2009).
[3]A. Najafi and R. Zargar, "Two-sphere low-Reynolds-number propeller," Phys. Rev. E **81**(6), 067301 (2010).
[4]A. Najafi and R. Golestanian, "Propulsion at low Reynolds number," J. Phys.: Condens. Matter **17**(14), S1203 (2005).
[5]J. J. Li and W. Tan, "A single DNA molecule nanomotor," Nano Lett. **2**(4), 315–318 (2002).
[6]I. Buttinoni, G. Volpe, F. Kümmel, G. Volpe, and C. Bechinger, "Active Brownian motion tunable by light," J. Phys.: Condens. Matter **24**(28), 284129 (2012).
[7]J. Palacci, S. Sacanna, S.-H. Kim, G.-R. Yi, D. J. Pine, and P. M. Chaikin, "Light-activated self-propelled colloids," Philos. Trans. R. Soc., A **372**(2029), 20130372 (2014).
[8]M. N. Popescu, S. Dietrich, M. Tasinkevych, and J. Ralston, "Phoretic motion of spheroidal particles due to self-generated solute gradients," Eur. Phys. J. E **31**(4), 351–367 (2010).
[9]U. M. Córdova-Figueroa and J. F. Brady, "Osmotic propulsion: The osmotic motor," Phys. Rev. Lett. **100**, 158303 (2008).
[10]F. Jülicher and J. Prost, "Comment on osmotic propulsion: The osmotic motor," Phys. Rev. Lett. **103**, 079801 (2009).
[11]E. M. Purcell, "Life at low Reynolds number," Am. J. Phys. **45**(1), 3–11 (1977).
[12]A. Najafi and R. Golestanian, "Simple swimmer at low Reynolds number: Three linked spheres," Phys. Rev. E **69**(6), 062901 (2004).

[13]W. F. Paxton, K. C. Kistler, C. C. Olmeda, A. Sen, S. K. St. Angelo, Y. Cao, T. E. Mallouk, P. E. Lammert, and V. H. Crespi, "Catalytic nanomotors: Autonomous movement of striped nanorods," J. Am. Chem. Soc. **126**(41), 13424–13431 (2004).
[14]T. R. Kline, W. F. Paxton, T. E. Mallouk, and A. Sen, "Catalytic nanomotors: Remote-controlled autonomous movement of striped metallic nanorods," Angew. Chem. **117**(5), 754–756 (2005).
[15]J. R. Howse, R. A. L. Jones, A. J. Ryan, T. Gough, R. Vafabakhsh, and R. Golestanian, "Self-motile colloidal particles: From directed propulsion to random walk," Phys. Rev. Lett. **99**(4), 048102 (2007).
[16]W. Gao, A. Pei, and J. Wang, "Water-driven micromotors," ACS Nano **6**(9), 8432–8438 (2012).
[17]W. Gao, R. Dong, S. Thamphiwatana, J. Li, W. Gao, L. Zhang, and J. Wang, "Artificial micromotors in the mouses stomach: A step toward *in vivo* use of synthetic motors," ACS Nano **9**(1), 117–123 (2015).
[18]A. Brown and W. Poon, "Ionic effects in self-propelled Pt-coated Janus swimmers," Soft Matter **10**(22), 4016–4027 (2014).
[19]S. Ebbens, D. A. Gregory, G. Dunderdale, J. R. Howse, Y. Ibrahim, T. B. Liverpool, and R. Golestanian, "Electrokinetic effects in catalytic Pt-insulator Janus swimmers," EPL **106**(5), 58003 (2014).
[20]S. J. Ebbens and J. R. Howse, "Direct observation of the direction of motion for spherical catalytic swimmers," Langmuir **27**(20), 12293–12296 (2011).
[21]L. Baraban, D. Makarov, R. Streubel, I. Monch, D. Grimm, S. Sanchez, and O. G. Schmidt, "Catalytic Janus motors on microfluidic chip: Deterministic motion for targeted cargo delivery," ACS Nano **6**(4), 3383–3389 (2012).
[22]S. Sundararajan, P. E. Lammert, A. W. Zudans, V. H. Crespi, and A. Sen, "Catalytic motors for transport of colloidal cargo," Nano Lett. **8**(5), 1271–1276 (2008).
[23]D. Patra, S. Sengupta, W. Duan, H. Zhang, R. Pavlick, and A. Sen, "Intelligent, self-powered, drug delivery systems," Nanoscale **5**(4), 1273–1283 (2013).
[24]Y. Wu, X. Lin, Z. Wu, H. Mohwald, and Q. He, "Self-propelled polymer multilayer Janus capsules for effective drug delivery and light-triggered release," ACS Appl. Mater. Interfaces **6**(13), 10476–10481 (2014).
[25]D. Kagan, R. Laocharoensuk, M. Zimmerman, C. Clawson, S. Balasubramanian, D. Kang, D. Bishop, S. Sattayasamitsathit, L. Zhang, and J. Wang, "Rapid delivery of drug carriers propelled and navigated by catalytic nanoshuttles," Small **6**(23), 2741–2747 (2010).
[26]F. Mou, C. Chen, Q. Zhong, Y. Yin, H. Ma, and J. Guan, "Autonomous motion and temperature-controlled drug delivery of Mg/Pt-poly (N-isopropylacrylamide) Janus micromotors driven by simulated body fluid and blood plasma," ACS Appl. Mater. Interfaces **6**(12), 9897–9903 (2014).
[27]Y. Gao and Y. Yu, "How half-coated Janus particles enter cells," J. Am. Chem. Soc. **135**(51), 19091–19094 (2013).
[28]L. Soler, V. Magdanz, V. M. Fomin, S. Sanchez, and O. G. Schmidt, "Self-propelled micromotors for cleaning polluted water," ACS Nano **7**(11), 9611–9620 (2013).
[29]B. Jurado-Sánchez, S. Sattayasamitsathit, W. Gao, L. Santos, Y. Fedorak, V. V. Singh, J. Orozco, M. Galarnyk, and J. Wang, "Self-propelled activated carbon Janus micromotors for efficient water purification," Small **11**(4), 499–506 (2015).
[30]D. Kagan, P. Calvo-Marzal, S. Balasubramanian, S. Sattayasamitsathit, K. Manian Manesh, G.-U. Flechsig, and J. Wang, "Chemical sensing based on catalytic nanomotors: Motion-based detection of trace silver," J. Am. Chem. Soc. **131**(34), 12082–12083 (2009).
[31]A. Walther and A. H. E. Müller, "Janus particles," Soft Matter **4**(4), 663–668 (2008).
[32]S. Michelin and E. Lauga, "Phoretic self-propulsion at finite Péclet numbers," J. Fluid Mech. **747**, 572–604 (2014).
[33]J. L. Moran, P. M. Wheat, and J. D. Posner, "Locomotion of electrocatalytic nanomotors due to reaction induced charge autoelectrophoresis," Phys. Rev. E **81**(6), 065302 (2010).
[34]Y. Daghighi and D. Li, "Micro-valve using induced-charge electrokinetic motion of Janus particle," Lab Chip **11**(17), 2929–2940 (2011).
[35]N. Sharifi-Mood, J. Koplik, and C. Maldarelli, "Diffusiophoretic self-propulsion of colloids driven by a surface reaction: The sub-micron particle regime for exponential and van der Waals interactions," Phys. Fluids **25**(1), 012001 (2013).
[36]W. E. Uspal, M. N. Popescu, S. Dietrich, and M. Tasinkevych, "Self-propulsion of a catalytically active particle near a planar wall: From reflection to sliding and hovering," Soft Matter **11**(3), 434–438 (2015).
[37]D. G. Crowdy, "Wall effects on self-diffusiophoretic Janus particles: A theoretical study," J. Fluid Mech. **735**, 473–498 (2013).
[38]A. E. Frankel and A. S. Khair, "Dynamics of a self-diffusiophoretic particle in shear flow," Phys. Rev. E **90**(1), 013030 (2014).
[39]A. Najafi and R. Golestanian, "Coherent hydrodynamic coupling for stochastic swimmers," EPL **90**(6), 68003 (2010).
[40]M. Farzin, K. Ronasi, and A. Najafi, "General aspects of hydrodynamic interactions between three-sphere low-Reynolds-number swimmers," Phys. Rev. E **85**(6), 061914 (2012).
[41]C. M. Pooley, G. P. Alexander, and J. M. Yeomans, "Hydrodynamic interaction between two swimmers at low Reynolds number," Phys. Rev. Lett. **99**(22), 228103 (2007).
[42]S. Childress, M. Levandowsky, and E. A. Spiegel, "Pattern formation in a suspension of swimming microorganisms: Equations and stability theory," J. Fluid Mech. **69**(03), 591–613 (1975).
[43]C. Dombrowski, L. Cisneros, S. Chatkaew, R. E. Goldstein, and J. O. Kessler, "Self-concentration and large-scale coherence in bacterial dynamics," Phys. Rev. Lett. **93**(9), 098103 (2004).
[44]A. Baskaran and M. Cristina Marchetti, "Statistical mechanics and hydrodynamics of bacterial suspensions," Proc. Natl. Acad. Sci. U. S. A. **106**(37), 15567–15572 (2009).
[45]Y. Hatwalne, S. Ramaswamy, M. Rao, and R. Aditi Simha, "Rheology of active-particle suspensions," Phys. Rev. Lett. **92**(11), 118101 (2004).
[46]M. Moradi and A. Najafi, "Rheological properties of a dilute suspension of self-propelled particles," EPL **109**(2), 24001 (2015).
[47]L. D. Landau and E. M. Lifshitz, *Fluid Mechanics*, Course of Theoretical Physics Vol. 6 (Butterworth-Heineman Ltd., 1987), pp. 227–229.
[48]H. Ohshima, *Theory of Colloid and Interfacial Electric Phenomena* (Academic Press, 2006), Vol. 12.
[49]O. Schnitzer and E. Yariv, "Osmotic self-propulsion of slender particles," Phys. Fluids **27**(3), 031701 (2015).
[50]E. Yariv, "Electrokinetic self-propulsion by inhomogeneous surface kinetics," Proc. R. Soc. A **467**, 1645 (2010).
[51]D. C. Prieve, J. L. Anderson, J. P. Ebel, and M. E. Lowell, "Motion of a particle generated by chemical gradients. Part 2. Electrolytes," J. Fluid Mech. **148**, 247–269 (1984).
[52]J. Happel and H. Brenner, *Low Reynolds Number Hydrodynamics: With Special Applications to Particulate Media* (Springer Science & Business Media, 2012), Vol. 1.
[53]S. Hosseini Rad and A. Najafi, "Hydrodynamic interactions of spherical particles in a fluid confined by a rough no-slip wall," Phys. Rev. E **82**(3), 036305 (2010).